Improved radiation tolerance of MAPS using a depleted epitaxial layer

A. Dorokhov*[,a], G. Bertolone[a], J. Baudot[a], A.S. Brogna[a], C. Colledani[a], G. Claus[a], R. De Masi[a], M. Deveaux[b], G. Dozière[a], W. Dulinski[a], J.-C. Fontaine[c], M. Goffe[a], A. Himmi[a], Ch. Hu-Guo[a], K. Jaaskelainen[a], M. Koziel[a], F. Morel[a], C. Santos[a], M. Specht[a], I. Valin[a], G. Voutsinas[a], F.M. Wagner[d], M. Winter[a]

[a] *Institut Pluridisciplinaire Hubert Curien (IPHC), 23 rue du loess, BP 28, Strasbourg, France 67037*
[b] *Goethe-Universität Frankfurt am Main, Senckenberganlage 31, Frankfurt am Main, Germany 60325*
[c] *Groupe de Recherche en Physique des Hautes Energies (GRPHE), Université de Haute Alsace, 61, rue Albert Camus, Mulhouse, France 68093*
[d] *Forschungsneutronenquelle Heinz Maier-Leibnitz (FRM II), Garching, Germany 85748*

Abstract

Tracking performances of Monolithic Active Pixel Sensors (MAPS) developed at IPHC [1] have been extensively studied [2], [3]. Numerous sensor prototypes, called MIMOSA[1], were fabricated and tested since 1999 in order to optimize the charge collection efficiency and power dissipation, to minimize the noise and to increase the readout speed.

The radiation tolerance was also investigated. The highest fluence tolerable for a 10 µm pitch device was found to be $\sim 10^{13}$ n_{eq}/cm^2, while it was only $2{\cdot}10^{12}$ n_{eq}/cm^2 for a 20 µm pitch device. The purpose of this paper is to show that the tolerance to non-ionising radiation may be extended up to $O(10^{14})$ n_{eq}/cm^2. This goal relies on a fabrication process featuring a 15 µm thin, high resistivity ($\sim$1 k$\Omega \cdot$ cm) epitaxial layer. A sensor prototype (MIMOSA-25) was fabricated in this process to explore its detection performances. The depletion depth of the epitaxial layer at standard CMOS voltages (< 5V) is similar to the layer thickness. Measurements with m.i.p.s[2] show that the charge collected in the seed pixel is at least twice larger for the depleted epitaxial layer than for the undepleted one, translating into a signal-to-noise ratio (SNR) of $\sim$ 50. Tests after irradiation have shown that this excellent performance is maintained up to the highest fluence considered ($3 \cdot 10^{13}$ n_{eq}/cm^2), making evidence of a significant extension of the radiation tolerance limits of MAPS.

Key words: Radiation Hardness, Monolithic Active Pixel Sensor, Tracking.
PACS: 29.40.Gx, 29.40.Wk, 61.80.-x

1. Introduction

A MAPS [1] is a semiconductor detector, which uses a matrix of p-n diodes (formed by N-well/P-epitaxial layer junctions in CMOS technology) as a sensing element. The charge liberated by the particle traversing the semiconductor volume is collected and transformed into signal by the readout electronics. The peculiarity of MAPS is that the readout electronics and sensing elements (N-well diode) are implemented in the same CMOS technology substrate (Fig. 1, left). This allows for a small pitch ($\sim$10 µm) and for a reduction of the equivalent noise charge (10 to 20 e), because the sensing element is located very close to the preamplifier. The standard CMOS technology substrate has very low resistivity (< 1 $\Omega \cdot$ cm), hence the epitaxial layer (typically 5-20 µm thick), featuring a relatively high resistivity ($\sim$10 $\Omega \cdot$ cm), is used as a sensing volume.

At standard CMOS voltages (< 5V), the depletion depth of the epitaxial layer is a fraction of micrometer (Fig. 1, right). The signal electrons get therefore predominantly collected through thermal diffusion. Non-ionising irradiation increases the trapping time for charge carriers in the epitaxial

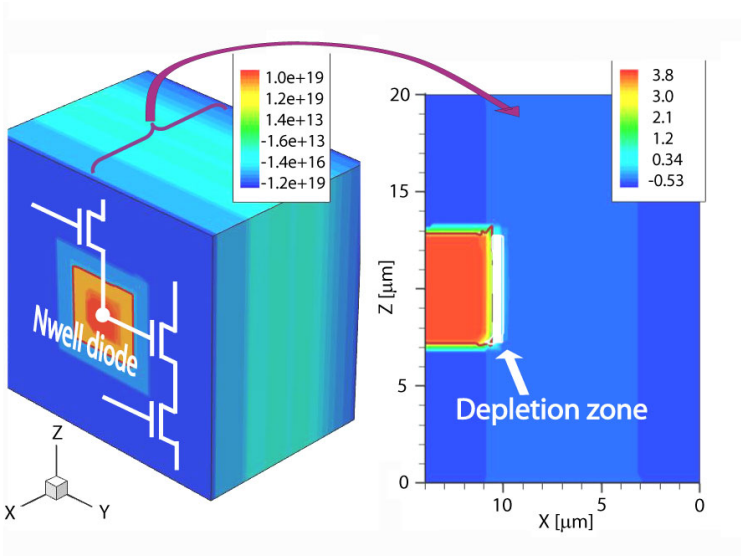

Figure 1: Left: N-well/P-epi diode connected to a 3 transistor pixel cell, in a low resistivity epitaxial layer. The color scale describes the doping concentration [cm^{-3}]. Right: Potential [V] calculated using Synopsys TCAD [4]. The white zone shows the depleted region.

*Corresponding author
Email address: Andrei.Dorokhov@IReS.in2p3.fr (A. Dorokhov)

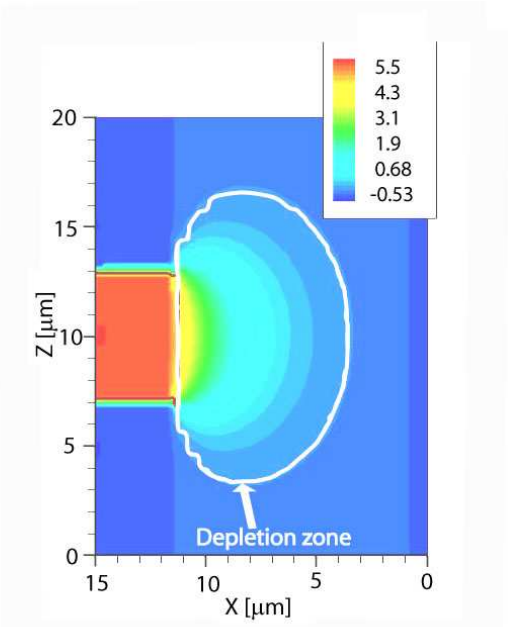

Figure 2: MAPS in a high resistivity epitaxial layer: potential [V] calculated using Synopsys TCAD [4]; The white curve surrounds the depleted region.

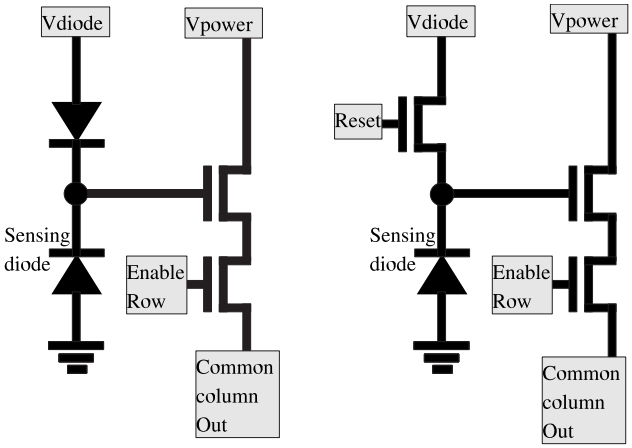

Figure 3: Schematic of pixels in the MIMOSA-25 chip: 3T with reset (right) and self biased with continuous reset (left).

layer; consequently, the signal charge collected may be reduced substantially [2], [3]. The need for industry to improve the performances of photo-detecting elements embedded in CMOS chips fostered the development of CMOS processes with special features [5]. These processes use a high resistivity epitaxial layer, which allows for a depletion depth of several micrometers (Fig. 2). Such a 0.6 micron technology has recently become available commercially [5]. It features a high resistivity ($\sim$1 k$\Omega \cdot$ cm), 15 μm thick, epitaxial layer. It was prototyped with a sensor (MIMOSA-25) and assessed with m.i.p.s.

2. Measurements and results

2.1. MIMOSA-25 sensor prototype

MIMOSA-25 contains two types of pixels: 3T with reset (Fig. 3 right) and self biased with continuous reset (Fig. 3 left). However, for simplicity, the "Reset" node was connected to "Vdiode" and all types of pixels were operated in continuous reset mode. The pixels have a 20, 30 or 40 μm pitch, and the sensing diodes' dimensions are 4×4 μm^2, 5×6.5 μm^2 or 11×11 μm^2. Each pixel type is reproduced in a matrix of 16 columns and 16-32 rows, depending on the pixel type. The smaller the pixel pitch, the smaller the probability for charge carriers to be trapped in the sensor bulk after irradiation. The smallest pitch (20 μm) was therefore chosen for the irradiation tests. The irradiation was performed with 1 MeV reactor neutrons. The fluences considered went up to $O(10^{14})$n$_{eq}$/cm^2.

2.2. Sensor calibration

The pitch is 20 μm for three matrices of 16 columns and 32 rows each. Two of these matrices feature a 3T pixel, one with 4×4 μm^2 sensing diodes (called[3] "RS 16 μm^2") and the other with 5×6.5 μm^2 sensing diodes (called "RS 32.5 μm^2"). The third matrix is composed of self-biased pixels, called "SB 32.5 μm^2". Each matrix is read out twice to perform correlated double sampling in order to remove the pedestal. The time between two successive readouts of the same pixel (coinciding with the charge integration time) is 76.8 μs and the measurements were done at +20°C.

The calibration of the readout gain is performed with an ^{55}Fe source, which emits X-Rays with energies of 5.9 keV and 6.5 keV. When the X-Ray energy is converted to charge carriers near the N-well of a sensing diode, the amplitude spectrum has a quite characteristic pattern, made of two peaks at the highest amplitudes of the spectrum (Fig. 4). Those peaks are used to calibrate the complete readout chain, allowing to convert the measurements with m.i.p.s into electron charge units at the input of the sensing diode. From Fig. 4 one can see that the "RS 16 μm^2" has peaks at the highest amplitudes, reflecting the diode size, i.e. the capacitance, which is the smallest implemented in the sensor. The matrices "RS 32.5 μm^2" and "SB 32.5 μm^2" have the same diode size, but the first matrix has peaks with smaller amplitudes. The reason is that the parasitic capacitance of the reset transistor (Fig. 3, right) is larger than the one of the forward biased diode (Fig. 3, left). Fig. 4 also displays the charge collected with a chip exposed to 3·10^{13} n$_{eq}$/cm^2. The amplitudes of the calibration peaks slightly differ from those of the non-irradiated chip. The difference is however comparable to the chip to chip gain variation, and can therefore not be attributed to irradiation. The calibration procedure above has been performed with all chips tested in order to convert the response to a ^{106}Ru source from ADC units to units of electron charge. The calibration uncertainty amounts to a few percents.

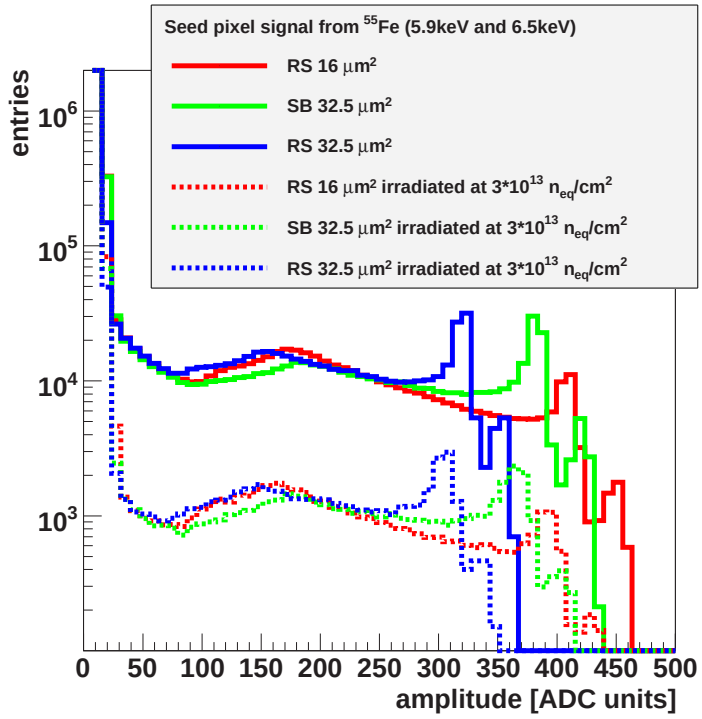

Figure 4: Charge collected in the seed pixel of MIMOSA-25 before irradiation and after an exposure to neutrons equivalent to $3{\cdot}10^{13}$ n_{eq}/cm^2. The 5.9 and 6.5 keV energy peaks from ^{55}Fe are clearly visible at the highest amplitudes. They are used to calibrate the gain. The entries in the histograms are scaled arbitrarily for the sake of clarity.

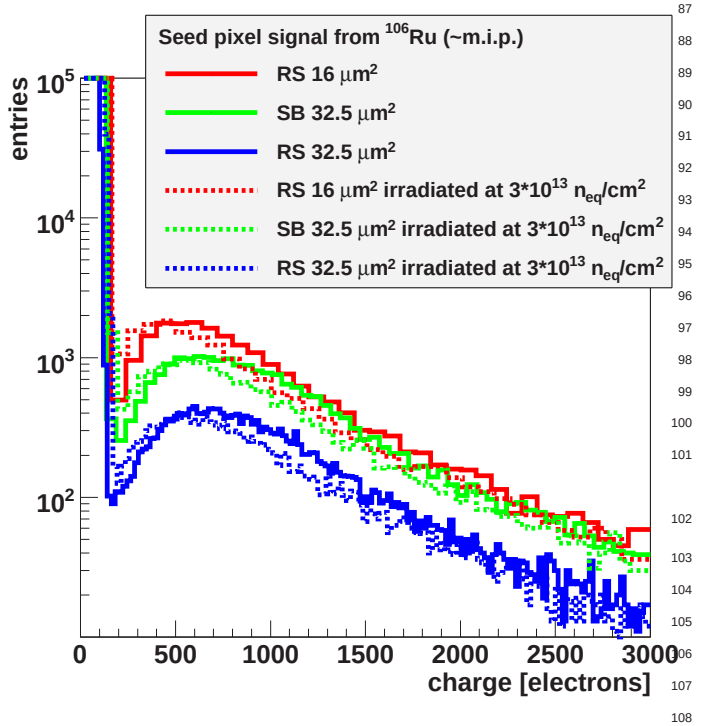

Figure 5: Charge collected in the seed pixel of MIMOSA-25 before irradiation and after an exposure to neutrons equivalent to $3{\cdot}10^{13}$ n_{eq}/cm^2.

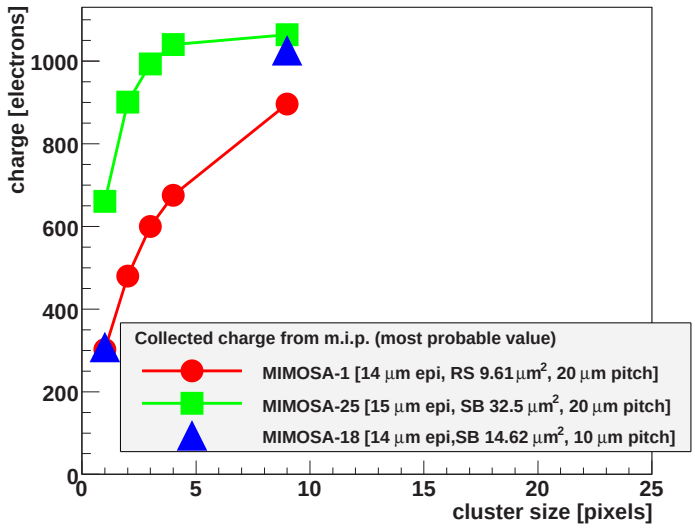

Figure 6: Charge collected in a cluster of pixels of the MIMOSA-25 (20 μm pitch) sensor implemented in a high resistivity epitaxial layer, compared to MIMOSA-1 (20 μm pitch) and MIMOSA-18 (10 μm pitch), implemented in a low resistivity epitaxial layer.

2.3. *Sensor response to a* ^{106}Ru *source*

Electrons emitted by a ^{106}Ru source were used to measure the sensor charge collection properties for m.i.p.s. The electrons traverse the sensor with about normal incidence and generate pixel clusters, out of which the pixel delivering the largest signal is called "seed pixel". The distribution of the charge collected in the latter is displayed in Fig. 5. Since no cut was applied on the charge value, the peak corresponding to thermal noise is clearly visible at low values. For larger values, one observes a typical Landau distribution expressing the signal charge generation. The most probable value (m.p.v.) of the distribution was used to evaluate the charge collection efficiency of the sensors. The total uncertainty on the m.p.v. was estimated to a few percent. The main message delivered by Fig. 5 is that a fluence of $3{\cdot}10^{13}$ n_{eq}/cm^2 affects only mildly the charge collected, which decreases by $\lesssim 10$ %.

The variation of the charge collected with the sensing diode geometry follows the expectations, i.e. it is ~ 20 % smaller for the smallest diode, and is identical in case of the two largest diodes. This remains true after irradiation.

2.4. *Radiation tolerance assessment*

Fig. 6 shows how the charge collection improves when using a depleted epitaxial layer instead of an undepleted one. The latter case is illustrated with two sensors fabricated several years ago: MIMOSA-1 (20 μm pitch) and MIMOSA-18 (10 μm pitch). MIMOSA-1 was chosen because it features the same pixel pitch as MIMOSA-25, while MIMOSA-18 is the

[3] In the names: RS (Reset type) or SB (Self-biased type), the number after the type is the N-well diode surface in micrometers squared.

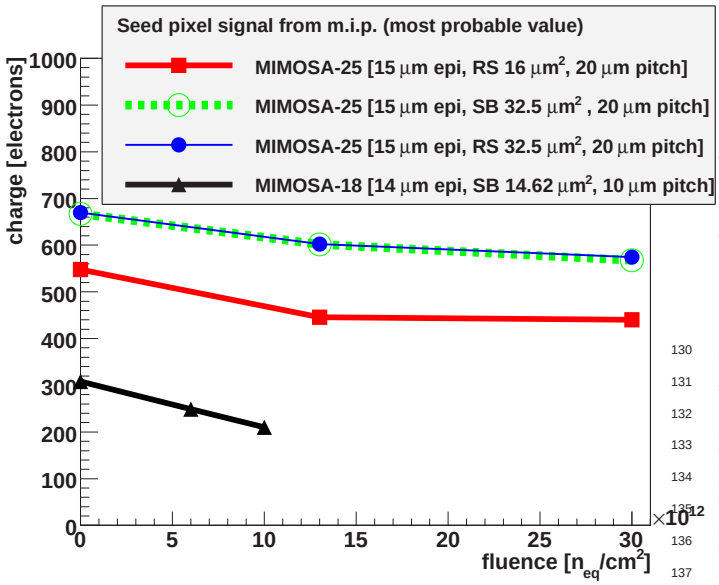

Figure 7: Charge in the seed pixel (m.p.v.) as a function of fluence: MIMOSA-25 with high resistivity epitaxial layer, MIMOSA-18 with low resistivity epitaxial layer.

MIMOSA-25	non-irradiated		$3 \cdot 10^{13}$ n_{eq}/cm^2	
	noise [e]	SNR	noise [e]	SNR
"RS 16 μm²"	10.8	50.6	14.7	30.0
"SB 32.5 μm²"	11.6	57.7	16.2	35.1
"RS 32.5 μm²"	13.3	50.3	18.9	30.4

Table 1: MIMOSA-25: the noise [e] and the signal-to-noise ratio (m.p.v.) before and after non-ionising radiation ($3 \cdot 10^{13}$ n_{eq}/cm^2).

most tolerant to non-ionising radiation up to now, due to its small pitch. The figure displays the charge collected for various pixel multiplicities inside a cluster, the pixels being ranked according to the fraction of the cluster charge they have collected. The value "1" thus corresponds to the seed pixel. One observes that the charge it collects is about twice larger for the depleted epitaxial layer (MIMOSA-25). The cluster charge is also much less spread ($\gtrsim$ 90 % of the cluster charge is concentrated in 3 pixels).

Fig. 7 shows the charge collected in the seed pixel (m.p.v.) for both layer types as a function of the fluence. The undepleted case is illustrated with MIMOSA-18 (taken from [6]). Values of the noise and SNR for non-irradiated and irradiated sensors are provided in Table 1.

MIMOSA-25 chips have been recently tested with pions of 120 GeV/c at the CERN-SPS. The preliminary results, briefly shown in Table 2, are in good agreement with those from the ^{106}Ru source (Fig. 7).

3. Discussion of the results

The charge collected in seed pixels (Fig. 6) of MIMOSA-25 is at least twice larger than in sensors with an undepleted epitaxial layer. This translates into a high SNR, of up to ~ 50 (m.p.v.). Another important advantage of the depleted layer is a faster collection time, which enhances the tolerance to non-ionising radiation. This is illustrated by the excellent detection performance of MIMOSA-25 after an exposure to neutrons equivalent to $3{\cdot}10^{13}$ n_{eq}/cm^2. The SNR is still ~ 35 for the "SB 32.5 μm²" pixel of MIMOSA-25, while it is only ~ 15 after a fluence of $1{\cdot}10^{13}$ n_{eq}/cm^2 for a 10 μm pitch sensor with undepleted epitaxial layer (MIMOSA-18). For a sensor prototype with the same low resistivity epitaxial layer but a 20 μm pitch (called MIMOSA-15), the SNR is already down to ~ 15 [7] for a still smaller fluence ($0.2{\cdot}10^{13}$ n_{eq}/cm^2). Considering sensors with identical pitch, present measurements show that those with depleted epitaxial layer exhibit a twice larger SNR than with an undepleted layer, after a fluence which is a factor of 15 higher. It is therefore likely that fluences in the order of 10^{14} n_{eq}/cm^2 are still affordable, i.e. 1-2 orders of magnitude beyond the limit observed with low resistivity epitaxial layers.

MIMOSA-25	non-irradiated	$3 \cdot 10^{13}$ n_{eq}/cm^2
"RS 16 μm²"	544 e^-	421 e^-
"SB 32.5 μm²"	647 e^-	513 e^-
"RS 32.5 μm²"	653 e^-	530 e^-

Table 2: MIMOSA-25 response to 120 GeV/c pions (CERN-SPS): charge collected in seed pixel (m.p.v.) measured with a non-irradiated chip and with one exposed to $3 \cdot 10^{13}$ n_{eq}/cm^2. A total uncertainty of a few percent affects all values displayed.

4. Conclusion and perspectives

The industrial need to improve of the photo-detectors embedded in a CMOS chip originated the access to a high resistivity epitaxial layer, instead of the standard, low resistivity, CMOS substrate. This high resistivity layer can be depleted at a standard CMOS voltage, which opens up new perspectives for MAPS.

The first sensor prototype fabricated with such a process has shown that this technological evolution will substantially improve the radiation tolerance of MAPS (by 1-2 orders of magnitude, up to $O(10^{14})$ n_{eq}/cm^2).

The feature size of the technology utilized for prototyping (0.6 μm) hampers however the design of complex MAPS with integrated signal processing. This is where 3D integration techniques, which allow combining different technologies, provide a very attractive solution. Moreover, technologies with a smaller feature size and with a similar high resistivity epitaxial layer are expected to become commercially available rather soon. It is thus likely that CMOS pixel sensors will be used in the mid-term for applications which look presently out of reach of this technology.

References

[1] A monolithic active pixel sensor for charged particle tracking and imaging using standard VLSI CMOS technology, R. Turchetta et al., Nucl. Instr. & Meth. in Phys. Res. Sect. A 458 (2001) 677-689.

[2] Achievements of the First Generation of Monolithic Active Pixel Sensor for Charged Particle Tracking, M. Winter et al., International Conference on High Energy Physics, 12-18 July 2001, Hungary.
[3] Test results of monolithic active pixel sensors for charged particle tracking, Yu. Gornushkin et al., Nucl. Instr. & Meth. in Phys. Res. Sect. A 478 (2002) 311-315.
[4] Process and Device Simulation Tools, Synopsys, Inc., Mountain View, California.
[5] Integrated PIN Photodiodes in High-Performance BiCMOS Technology, M. Förtsch et al., Electron Devices Meeting, 2002. IEDM '02. Digest. International.
[6] CMOS Pixel Sensors for Charged Particle Tracking: Achieved Performances and Perspectives, M. Winter, 1st international conference on Technology and Instrumentation in Particle Physics, 2009, Tsukuba, Japan.
[7] Charge collection properties of Monolithic Active Pixel Sensors (MAPS) irradiated with non-ionising radiation, M. Deveaux et al., Nucl. Instr. & Meth. in Phys. Res. Sect. A 583 (2007) 134-138.